Structural and Spectroscopic Properties of Mg−Bacteriochlorin and Methyl Bacteriochlorophyllides *a*, *b*, *g*, and *h* Studied by Semiempirical, ab Initio, and Density Functional Molecular Orbital Methods

Juha Linnanto and Jouko Korppi-Tommola*

Department of Chemistry, University of Jyväskylä, P.O. Box 35, FIN-40014 Finland

Received: August 15, 2003; In Final Form: December 1, 2003

Ab initio HF/6-31G* and density functional B3LYP/6-31G* methods have been used to calculate fully optimized structures of methyl bacteriochlorophyllides *a*, *b*, *g*, and *h* and magnesium-bacteriochlorin. Semiempirical ZINDO/S CIS and ab initio CIS/6-31G* and CIS/6-311G** configuration interaction methods and time dependent HF/6-31G*, HF/6-311G**, B3LYP/6-31G*, and B3LYP/6-311G** methods were used to estimate corresponding spectroscopic transition energies of the chromophores. The effects of solvent coordination were also studied by optimizing structures of 1:1 complexes of the methyl bacteriochlorophyllides and acetone. The self-consistent reaction field model was used to estimate bulk solvent effects. Differences in B3LYP and HF bond lengths of the bacteriochlorin had a strong influence on the calculated transition energies. Large variations of calculated transition energies were also observed when coordinates from different X-ray structure determinations were used for the same pigment. In the five coordinated solvent complex, the Mg atom is shifted from the bacteriochlorin plane, inducing red shifts of the Q_x and Soret transitions. Linear correlations of the calculated and experimental solution transition energies were obtained with characteristic slopes and intercepts for each method used, reflecting inadequacy of the methods to describe transition energies in bacteriochlorins. Such correlations were shown to be useful in prediction of site transition energies for a pigment (pigment group) in solution or in protein under a given computational approach. Best correlations and the best calculated transition energies were obtained by using the ZINDO/S CIS method with B3LYP/6-31G* optimized structures. Calculations suggested the existence of a number of dark electronic states of bacteriochlorophylls below the main Soret transition. The density of these states was dependent on pigment surroundings. Dark states may have an important role in carotenoid to chlorophyll or to bacteriochlorophyll energy transfer in photosynthetic light harvesting complexes. It was also shown that conformation of an acetyl group of methyl bacteriochlorophyll *a* has an effect on calculated transition energies.

1. Introduction

Magnesium−bacteriochlorin (Mg−bacteriochlorin, Mg−BC) types bacteriochlorophylls (Bchls) *a*, *b*, and *g* are pigments that take part in the photosynthetic processes in purple, green sulfur, green non-sulfur, and heliobacteria.[1] They play two roles in photosynthetic protein complexes: they collect and funnel light energy and serve as electron carriers in the reaction centers.[1,2] Structural determinations of the photosynthetic pigment−protein complexes provide detailed knowledge of the organization of pigment molecules in the photosynthetic membranes.[3−9] Experimental crystal structures of photosynthetic complexes have made the use of quantum chemical molecular orbital calculations possible for investigation of various molecular mechanisms of photosynthesis.[10−49] However, the size of pigment−protein complexes puts restrictions on the use of quantum chemical methods. In practice, it is feasible to do calculations to model systems containing a few hundred atoms. This means that a calculation may contain only one or two photosynthetic chromophores and sometimes also their nearest environment. The rest of the molecular system has to be ignored.[24−49] It is very important to choose a model system that is representative enough to contain all of the necessary information about the real system but which does not put constraints that are too heavy on the computations. The quality (resolution) of the experimental structure used for modeling is another important factor. A very good resolution of X-ray structures of photosynthetic protein complexes is about 2.0 Å. Poorer quality of coordinates may introduce severe errors on calculated transition energies which are comparable to those obtained from the use of coordinates from a "low level of theory". Quantum chemical molecular orbital methods have been used to calculate structures, vibrational frequencies, chemical shifts, and electronic properties of monomeric bacteriochlorophylls and their radicals in several previous studies.[50−67]

The aim of the present study was to find out how different quantum chemical molecular orbital methods predict structures and spectroscopic properties of monomeric methyl bacteriochlorophylls and their complexes. Also the influence of the surrounding environment on the structures and energy levels of the chromophores was studied. It was considered of importance to search for a computationally most efficient and reliable approach(es) from the large pool of methods available and to test their validity in describing in vivo pigment systems. Such tools are essential for reliable modeling of photosynthetic protein complexes. Influence of the conformation of the acetyl group of methyl bacteriochlorophyll *a* on calculated transition energies was studied. Structural differences obtained from different computational methods and from different X-ray

* To whom correspondence should be addressed.

10.1021/jp0309771 CCC: $27.50
Published on Web 06/16/2004

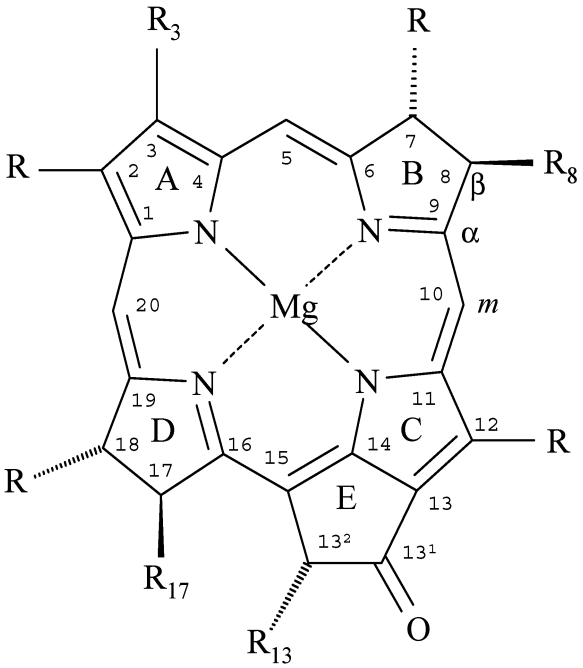

Figure 1. Model structure of the methyl bacteriochlorophylls. For description of the substituents, see Table 1.

TABLE 1: Description of Substituents of Individual Methyl Bacteriochlorophyllides and Mg-Bacteriochlorin[a]

molecule	R_3	R_8	R_{13}	R_{17}
Mg−BC[b]	−H	−H	−	−H
MeBchl *a*[c]	−CO−CH_3	−C_2H_5	−CO−O−CH_3	−C_2H_4−CO−O−R
MeBchl *b*[c]	−CO−CH_3	=CH−CH_3	−CO−O−CH_3	−C_2H_4−CO−O−R
MeBchl *g*[c]	−CH=CH_2	=CH−CH_3	−CO−O−CH_3	−C_2H_4−CO−O−R
MeBchl *h*[c]	−CH=CH_2	−C_2H_5	−CO−O−CH_3	−C_2H_4−CO−O−R

[a] For basic structure see Figure 1. [b] Without ring E and R is H-atom. [c] R is CH_3.

determinations were compared and their influence on transition energies studied.

2. Chromophores and Computational Methods

Methyl bacteriochlorophyllides (MeBchls) *a*, *b*, *g*, and *h* were used as model structures for Bchls *a*, *b*, *g*, and *h*. The difference between chemical structure of Bchls and MeBchls is the length of the hydrocarbon tail in position R17 (MeBchls contain methyl instead of phytyl or farnesyl). Chemical structures of the MeBchls studied are described in Figure 1 and in Table 1. A common feature of all studied structures is that the bacteriochlorin ring consists of two pyrroline (the B and D rings) and two pyrrole (the A and C rings) rings. The studied MeBchls differ in structure with respect to substitutions in R3 and R8 positions. MeBchl *a* contains an acetyl group at the R3 position and an ethyl group at the R8 position; in MeBchl *b*, the same positions are occupied by an acetyl and ethyldiene, in MeBchl *g* by vinyl and ethyldiene, and in MeBchl *h* by ethyldiene and ethyl groups, respectively.[29] Bchl *a*, *b*, and *g* are found in photosynthetic bacteria, but Bchl *h*, the vinyl substituted analogue of Bchl *a*, is an as-yet undiscovered compound as also its spectroscopic properties.[29]

The monomer structures of MeBchl *a*, *b*, *g*, and *h* and Mg−BC (Figure 1 and Table 1) were fully optimized at the ab initio HF/6-31G* level and the density functional B3LYP/6-31G* level on an AlphaServer ES-40 and Silicon Graphics Onyx2 workstations by using the Gaussian 98 software.[68] Optimized monomer geometry was used in the calculation of atomic charges (Mulliken population analysis), transition energies, and oscillation strengths. The atomic charges were calculated at the ab initio Hartree−Fock level and the density functional B3LYP level by using the 6-31G* basis set. Geometry optimizations of the 1:1 complexes of the MeBchls and acetone were done at HF/6-31G* and B3LYP/6-31G* levels. Transition energies and oscillation strengths were calculated at semiempirical ZINDO/S CIS (40,40) or (45,45) levels by using ArgusLab (version 2.0.0) software running on a pentium PC.[69−72] The ZINDO/S CIS (40,40) with simple self-consistent reaction field (SCRF) method was also tested for its predictive power in estimation of electronic transition energies of the present chromophores and especially to study existence of dark electronic states in these systems.[73] A cavity radius of 8 Å that well covers the van der Waals surface of MeBchl was used in SCRF calculations. The dielectric constant of 20.7 and reflective index of 1.3588 for acetone solutions at 20 °C were used.[74] Ab initio CIS/6-31G* (5,5) or (6,6), CIS/6-311G** (5,5) or (6,6) and time dependent (TD) HF/6-31G*, HF/6-311G**, B3LYP/6-31G*, and B3LYP/6-311G** level calculations were carried out on a Silicon Graphics Onyx2 workstation.

TABLE 2: Comparison of Heavy Atom Bond Length Differences of the Bacteriochlorin Ring of Bacteriochlorophyll *a*[a]

structure	average deviation [Å]	standard deviation [Å]	maximum deviation [Å]
	calculated		
HF/B3LYP	0.032	0.019	0.067
PM3/B3LYP	0.062	0.055	0.346
PM5/B3LYP	0.029	0.019	0.075
	X-ray[b]		
2.8/1.9b	0.032	0.022	0.193
1.9a/1.9b	0.029	0.019	0.197

[a] Calculated structures: methyl bacteriochlorophyll *a* from PM3, PM5, and HF/6-31G* optimizations as compared to B3LYP/6-31G* structure. X-ray structures: Bchl *a1* of the FMO protein of *Prosthecochloris aestuarii* from different X-ray determinations.[7,133,135] [b] 2.8 Å resolution structure from Ref. (133) and 1.9 resolution structures from refs 7 and 135 for structures 1.9a and 1.9b, respectively.

3. Results and Discussions

3.1. Structure. Both computational methods, Hartree−Fock (HF) and Becke's three-parameter hybrid (B3LYP) functional, gave the structures in a vacuum where the four coordinated Mg atom of bacteriochlorin is located at the center and almost in the plane of the bacteriochlorin ring (Table 1S, supplementary information). This result is in agreement with several experimental X-ray structures of bacteriochlorophylls in protein and also with the results from semiempirical PM5 calculations for Chls and Bchls.[3,4,6,7,57,75−79] In Table 2 are shown average, standard, and maximum deviation for the bacteriochlorin ring bond lengths of MeBchl *a* optimized by PM3, PM5, and HF/6-31G* methods with respect to bond lengths obtained from B3LYP/6-31G* calculations. The methods used seem to give quite similar statistical data, only PM3 gives a little larger variation. The reason is that the PM3 calculation puts the magnesium atom clearly off the bacteriochlorin plane. Similar statistical data were obtained also for the other four pigments studied. The results for Chl *a* from our previous work[57] PM5, HF/6-31G*, and B3LYP/6-31G* point to the same direction with a maximum bond length difference about 0.05 Å, when compared to the X-ray structure of ethyl chlorophyllide *a*. Table 2 shows also that resolution differences in the experimental X-ray structure determinations give statistical errors that are

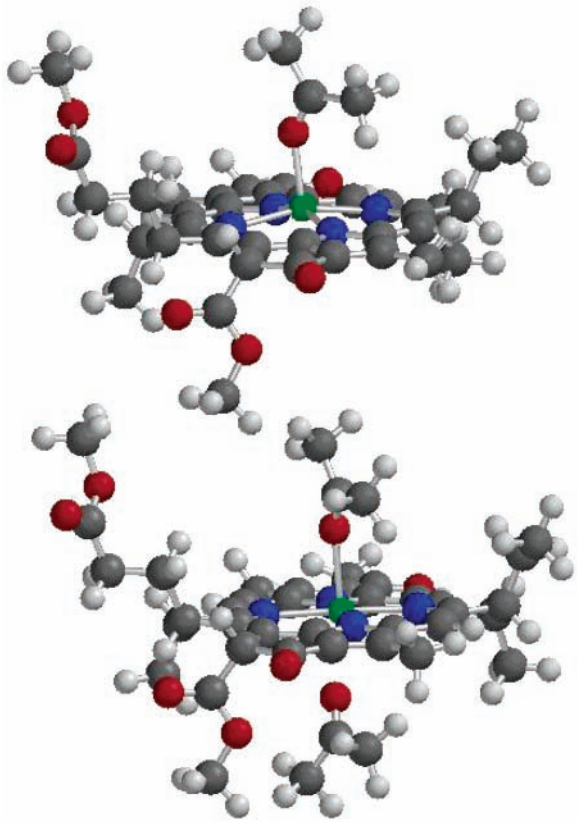

Figure 2. B3LYP/6-31G* optimized structures of methyl bacteriochlorophyll *a* acetone complexes, 1:1 complex (top) and 1:2 complex (bottom). Observe nonplanar bacteriochlorin structure of the 1:1 complex.

similar to those obtained from the various computationally optimized structures. Such structural differences have a strong effect on calculated transition energies as will be shown below.

In all modeled 1:1 acetone−MeBchl complexes, the Mg atom was about 0.36 Å (B3LYP) or 0.44 Å (HF) above the bacteriochlorin plane on the same side as the binding acetone (Figure 2). The semiempirical PM5 method gives a similar result.[57] It is then quite likely that the interaction between the polar solvent molecule and the magnesium atom of the bacteriochlorin is strong, and such a distorted bacteriochlorin structure is present and even dominant for Bchls in solution. The result is also in line with several X-ray structures of five coordinated bacteriochlorophyll type molecules.[4,6,7,79−84] In minimum energy structures of the 1:2 MeBchl−acetone complexes, the Mg atom was only about 0.1 Å above the bacteriochlorin plane on the side where the acetone is closer to bacteriochlorin, see Figure 2.

One major difference between the calculated and X-ray structure (ethyl chlorophyllide *a* dihydrate molecule[81]) became apparent (Table 1S, in the Supporting Information). In the calculated structures, the three bond lengths between carbons 6, 7, 8, and 9 are longer than the experimental reference values. These differences arise from different bonding in the B ring of the reference compound (pyrrole, chlorin ring) and the calculated MeBchls (pyrroline, bacteriochlorin ring).[81] Ethyl chlorophyllide *a* was used as the reference compound since there is no X-ray crystal structure for Mg−BC type bacteriochlorophylls in the protein-free environment. In the optimized Mg−BC structures, the $C_\beta - C_\beta$ bond of pyrroline is longer (B3LYP: 1.543 Å; HF: 1.535 Å) than the corresponding experimental bond in zinc tetraphenylbacteriochlorin (Zn-TPBC; 1.479−1.497 Å).[82] The structural differences of the two B rings are also reflected in the dihedral C6−C7−C8−C9 angle of MeBchls. In the pyrrole ring, this angle is almost zero, but in the optimized pyrroline ring, it is clearly nonzero. In Mg−BC, the planar B ring was predicted in accordance with the X-ray structure of Zn-TPBC.[82] It is noted that in the crystalline ethyl chlorophyllide *a* the Mg atom is five coordinated and magnesium is clearly above the chlorin plane, whereas in the optimized four coordinated structures, magnesium is in the bacteriochlorin plane.[81]

In general, the B3LYP/6-31G* method produced bond lengths slightly better than the HF/6-31G* method as has been previously shown for porphyrin and chlorin.[85] On the other hand, for Chl *a*, both methods gave a bond length maximum difference about 0.05 Å when compared to the X-ray structure.[57] The HF and B3LYP methods produce bacteriochlorin ring structures with alternating bond lengths, alternation being weaker in B3LYP optimized structures than in the HF optimized structures. The available crystal structure is consistent with the B3LYP results.[86−88] Different substituents in Chls and Bchls break the ideal conjugation of the porphyrin skeleton. This is evidenced also by X-ray and NMR studies of substituted porphyrins suggesting weak alteration of bond lengths and inequivalence of the carbon nuclei in the porphyrin skeleton, respectively.[82,89−93] The calculated HF and B3LYP bond lengths C7−C8 and C8−C9 are longer in Mg−BC and MeBchl *a* and *h* than the corresponding lengths in MeBchl *b* and *g*. The differences arise from different substituents at carbon C8, where MeBchl *a* and *h* has an ethyl group and MeBchl *b* and *g* an ethylidene group.

According to the B3LYP results, in all calculated structures, the $N-C_\alpha-C_m$ (e.g., NC−C14−C15, see definitions of α, *β*, and *m* in Figure 1) angles common to the rings C and E are largest, and the values vary between 133 and 134° (exp. 133.8°, experimental values below refer to ref 81). The other $N-C_\alpha-C_m$ angles were in the ranges 121−127° and 125−127° (exp. 121−125°) for MeBchls and Mg−BC, respectively, and $C_\alpha-C_m-C_\alpha$ angles were in the range 124−129° (exp. 126−129°). These results are in accord with previously reported values.[50,57,94,95] The $C_\alpha-N-C_\alpha$ angles of the A and C rings and the B and E rings were in the ranges 106−108° (exp. 106−108°) and 110−111° (exp. 109°), respectively. The values reflect the shorter bond length between C_β atoms in the A and C rings as compared to the same distance in the B and D rings (see Table 1S). The $C_\alpha-C_\beta-C_\beta$ angles in A and C rings vary between 104 and 107° (exp. 105−109°), and the $C_\alpha-C_\beta-C_\beta$ angles in B and E rings are in the range 102−103° (exp. 102−103°), except in MeBchl *b* and *g* in which the corresponding value for B ring was 106°. Both MeBchl *b* and *g* have an ethylidene group in position C8, which may be the reason for opening the $C_\alpha-C_\beta-C_\beta$ angle from about 102° in MeBchl *a* and *h* to 106° in MeBchl *b* and *g*. Both B3LYP/6-31G* and HF/6-31G* methods gave similar results for bond angles of MeBchls, the average difference between the two methods being less than 1%. The calculated values are in good agreement with the experimental X-ray structure of the ethyl chlorophyllide *a* dihydrate.[81]

In the B3LYP structures (both vacuum and 1:1 complexes), the dihedral angle C6−C7−C8−C9 (B ring) was about 19° for MeBchl *a* and *h* and about 8° for MeBchl *b* and *g*. The C16−C17−C18−C19 angle (D ring) was 16° (exp. 13.05°). This result is in disagreement with an ^{1}H NMR study for Bchl *a* in tetrahydrofuran-d_8, which suggested that the ring D is more buckled than the ring B.[90] In the HF optimized structures, the dihedral angles were 2−5° larger than in the B3LYP structures. According to HF and B3LYP optimizations, the Mg−BC is

planar in agreement with the X-ray structure of Zn−TPBC.[82] In the B3LYP optimized structures, the acetyl group at the R3 position is in the bacteriochlorin plane pointing toward the hydrogen in the C5 position but the ethenyl group is twisted out of plain (dihedral angle C2−C3−CR3−CR3′ is about 25°). In the HF optimized structures, both groups are twisted out of plain (dihedral angle C2−C3−CR3−CR3′ is about 40°). Such conformational differences might have strong effects on the Q_y transition energy as has been suggested in the literature.[11] In the experimental X-ray structures of Bchl *a* in protein, the acetyl group at position R3 is twisted out of plain in most cases.[4,7,8,96−99] The bacteriochlorin ring is almost planar according to B3LYP calculations but slightly curved in the HF structure. The Mg atom is about 0.03 and 0.18 Å above the plane defined by C_β carbons (C2, C8, C12, and C18) for B3LYP and HF structures, respectively. The planar structure of porphyrin is experimentally observed in chlorophyll like molecules.[79]

For the 1:1 complexes of MeBchl and acetone, both the HF and B3LYP methods gave structures, where the oxygen atom of acetone is noncovalently binding to the Mg atom of the bacteriochlorin resulting in an energy reduction of about 20 kcal/mol as compared to the isolated species (Figure 2). The result is in accordance with the experimental interpretation that in acetone solution the Mg atom of Chls and Bchls is five coordinated.[100−107] Calculations show that there is a small energy difference between the two binding sites of the 1:1 complexes. The energetically more favorable (about 2 kcal/mol) binding site is the one where acetone is on the same side with the R_{17} group. In several X-ray studies two binding sites of Bchls in protein have been identified.[4,6,7,79−84] In Figure 2 is also shown the structure of the 1:2 acetone complex. Its total energy is about 10 kcal/mol higher than that of the 1:1 acetone complex and isolated acetone plus binding energy (energy difference between 1:1 complex and isolated species).

The distance between the oxygen atom of acetone and the Mg atom of the bacteriochlorin is about 2.2 Å in all optimized HF and B3LYP structures (exp. 2.034 Å). The semiempirical PM5 method gave distances in the range of 2.0−2.2 Å.[57] In the 1:2 complex, the bonding distance of the energetically more favorable acetone (1:1 complex case) is 2.26 Å, whereas that of its counterpart is 2.4 Å. The C−O−Mg angle (i.e., C−O is C═O group of acetone) was about 146°. In all 1:1 complexes, one of the methyl groups of the binding acetone is directed toward the rings B and C, perturbing the electron density of this part of the bacteriochlorin ring. In the 1:1 complexes, the distances of the magnesium form the bacteriochlorin plane were about 0.45 Å (HF), 0.35 Å (B3LYP), and 0.40 Å (PM5) (exp. 0.385Å).[57] According to calculations complexation also distorts magnesium nitrogen binding symmetry and carbon−carbon bond lengths in the bacteriochlorin plane. This result is in agreement with a density functional study for Bchl and Chl water complexes[63] and also with a ^{13}C NMR study for chlorophyll *a* and pheophytin *a*, showing that solvent coordination changes ^{13}C chemical shifts of the porphyrin skeleton.[91]

3.2. Atomic Charges. The most important atomic charges (according to Mulliken population analysis) of MeBchls and Mg−BC are given in Table 3. Both HF and B3LYP methods give a positive charge on magnesium and negative charges for the N and O atoms. The HF charges are more than 30% more positive that the B3LYP charges. It is obvious then that estimation of Coulombic interaction energies of Bchls and Chls and their aggregates in proteins based on methods that rely on atomic charges are highly dependent on the level of calculations used to get the charges.[36] In 1:1 complexation of MeBchls and acetone, magnesium is receiving and NB, NC, and ND atoms are loosing negative charge as compared to vacuum charges. This effect is slightly stronger in HF than B3LYP charges. Also atomic charges of C atoms are reduced on complexation, especially the charges in the C and E rings (not shown). NMR results of acetone solution of Chl *a* indicate similar trends.[91] Observed charge redistributions suggest noncovalent binding of acetone with the Mg atom. Such noncovalent bonding mechanisms for Chls and Bchls in solution and in protein have been suggested in several structural and spectroscopic studies.[3,4,6,20,75,76,78,80,98,100−116]

According to Mulliken population analysis (B3LYP) of MeBchl *a* and *b* the hydrogen at position C5 is about 0.07 [e] more positive than the other C_m hydrogens. In the HF optimized MeBchl *a* and *b*, where the acetyl group at R3 was twisted about 40° out of plain and in the B3LYP optimized MeBchl *g* and *h* where the vinyl groups are twisted out of plane no significant charge differences between the C_m hydrogens was observed. Rotation of the acetyl group of MeBchl *a* at position R3 studied by B3LYP method shows similar results, increasing the dihedral angle C2−C3−CR3−CR3′ from 0 to ±40° decreases the charge difference between the C_m hydrogens. If the acetyl group at position R3 is pointing toward the hydrogen of C5 the electron density around hydrogen is reduced. A similar trend has been observed in a ^1H NMR study of Bchl *a* type metal-substituted Bchls, where the proton at position C5 showed a larger chemical shift than the other C_m protons.[117] Orientation of the acetyl group toward the proton of C5 may give rise to charge redistribution and to shielding effects.[118] Thus, the experimentally observed large chemical shift for the proton at the position C5 suggests a structure where the acetyl group is almost in the bacteriochlorin plane.

3.3. Transition Energies. Figure 3 visualizes calculated lowest energy transition energies of Mg−BC and the MeBchls in a vacuum and for 1:1 acetone complexes at various levels of calculation. In Tables 2S and 3S (Supporting Information) are tabulated corresponding calculated transition energies in eV units. Correlations between calculated (B3LYP optimized 1:1 acetone complexes) and experimental transition energies are shown in Figure 4. The experimental transition energies were taken as absorption band positions of monomeric Bchls in acetone or in diethyl ether at room temperature.[50] Least-squares fits were used to correlate experimental and calculated transition energies, as suggested by Petke at al.[58−60,119−122] The fitting parameters have been listed in Table 4S (Supporting Information). It is obvious from Table 4S that the fits in most cases do not represent an "ideal correlation" with a slope unity and intercept zero. There are two underlying reasons for such behavior; First, the behavior reflects inadequacy of the methods used to describe transition energies of the bacteriochlorins, and second, the experimental energies taken as solution band positions are not necessarily good enough as experimental reference for vacuum structures (though best available). However, existence of linear correlations means that transition energies obtained from such correlations may be used to estimate transition energies of real systems. It is possible to predict spectroscopic properties of structurally similar molecules such as Bchl *h* for which the spectroscopic data is not available. The values of slope and intercept reflect only the quality of the method used to reproduce the experimental energies. Petke's suggestion serves the need to make an estimation of transition energies of various porphyrines in various environments and with various computational methods possible in a systematic manner. Tables 4 and 5 summarize the results for the optically

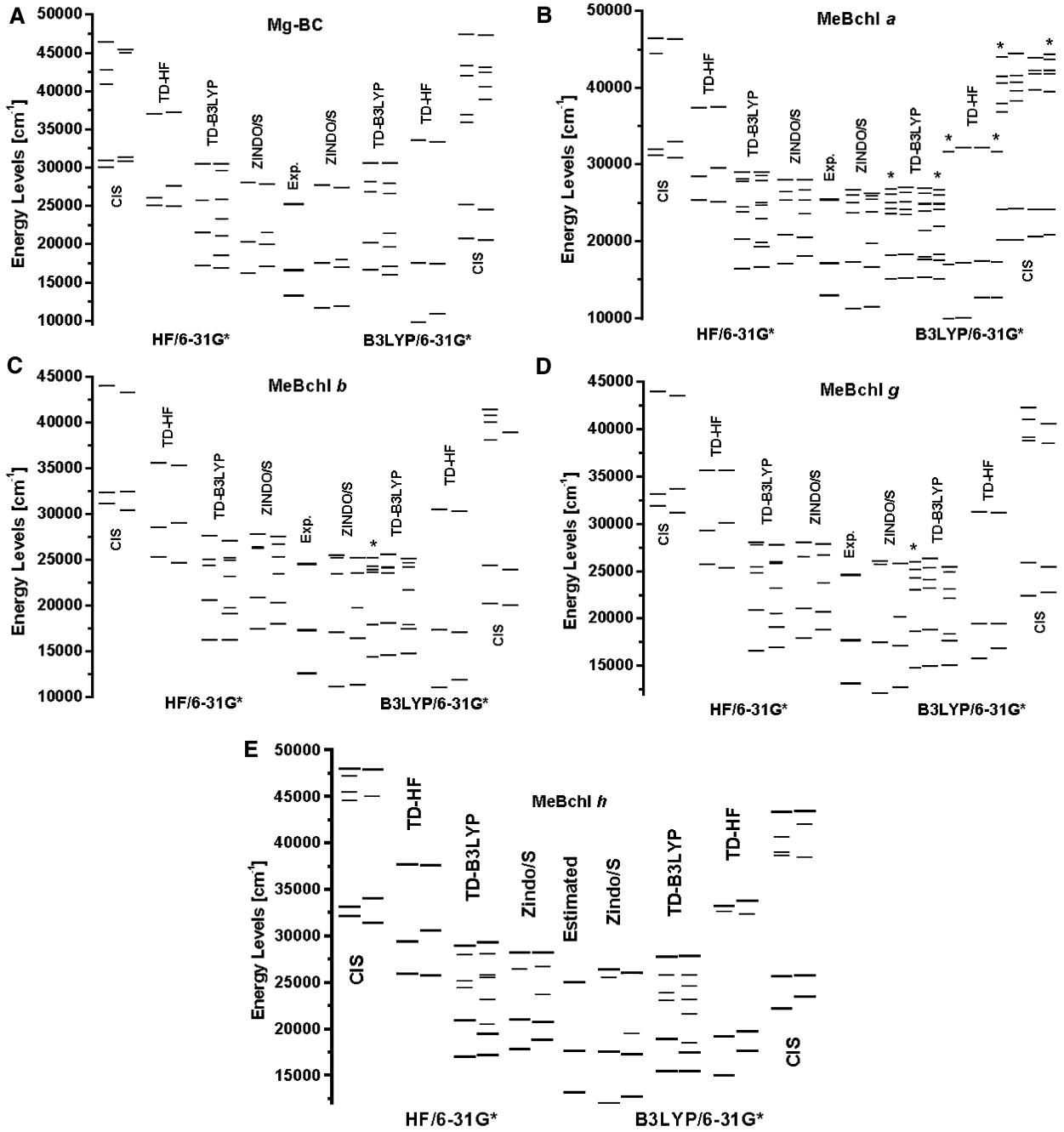

Figure 3. Energy level diagram's of magnesium bacteriochlorin and methyl bacteriochlorophylls. The levels on the left-hand side refer to HF/6-31G* geometries, and the levels on the right-hand side refer to B3LYP/6-31G* geometries. In the middle, experimental solution values are shown. Under each method label two energy level columns are given, the one on the left-hand side refers to a four coordinated pigment (vacuum) the one on the right to a five coordinated pigment (1:1 acetone complex). Starred energy level sets have been calculated by using the 6-311G** basis sets. Thinned gray lines refer to dark states below the main Soret transition. Three bold lines in each energy level column refer to Q_y, Q_x, and Soret levels, Q_y being lowest in energy.

allowed Q_y, Q_x, and Soret (B) transitions of the MeBchls and Mg−BC, which were estimated by using the parameters of Table 4S.

3.3.1. Excited-State Energy Levels. Optimized HF geometries of Mg−BC, MeBchls, and their 1:1 acetone complexes give much blue shifted calculated transition energies when compared to transition energies obtained from the B3LYP geometries, as may be seen from the energy level diagrams of Figure 3. An obvious explanation is that the HF method localizes the π electrons more than the DFT does, e.g., the bond alteration in the former is stronger that in the latter. From the diagrams it can be seen that complexation decreases energy difference between Q_y and Q_x levels and increases it between Q_x and Soret levels except for CIS and TD-HF energies of HF structures. Increasing the size of the basis set from 6-31G* to 6-311G** in the calculations seems to have little effect on the calculated transition energies (the energy level columns marked with *, Figure 3). The TD-B3LYP method especially gives a number of additional states below the main Soret transition (shorter gray lines). The ZINDO/S also produces such additional states but they are fewer in number. As shown in Figure 3, there are not large differences in the TD-B3LYP energies between HF and B3LYP optimized structures. Thus, the TD-B3LYP method is not as sensitive to differences in geometry as the other methods used.

In general, the calculated transition energies are systematically larger than the experimental solution values. This is not

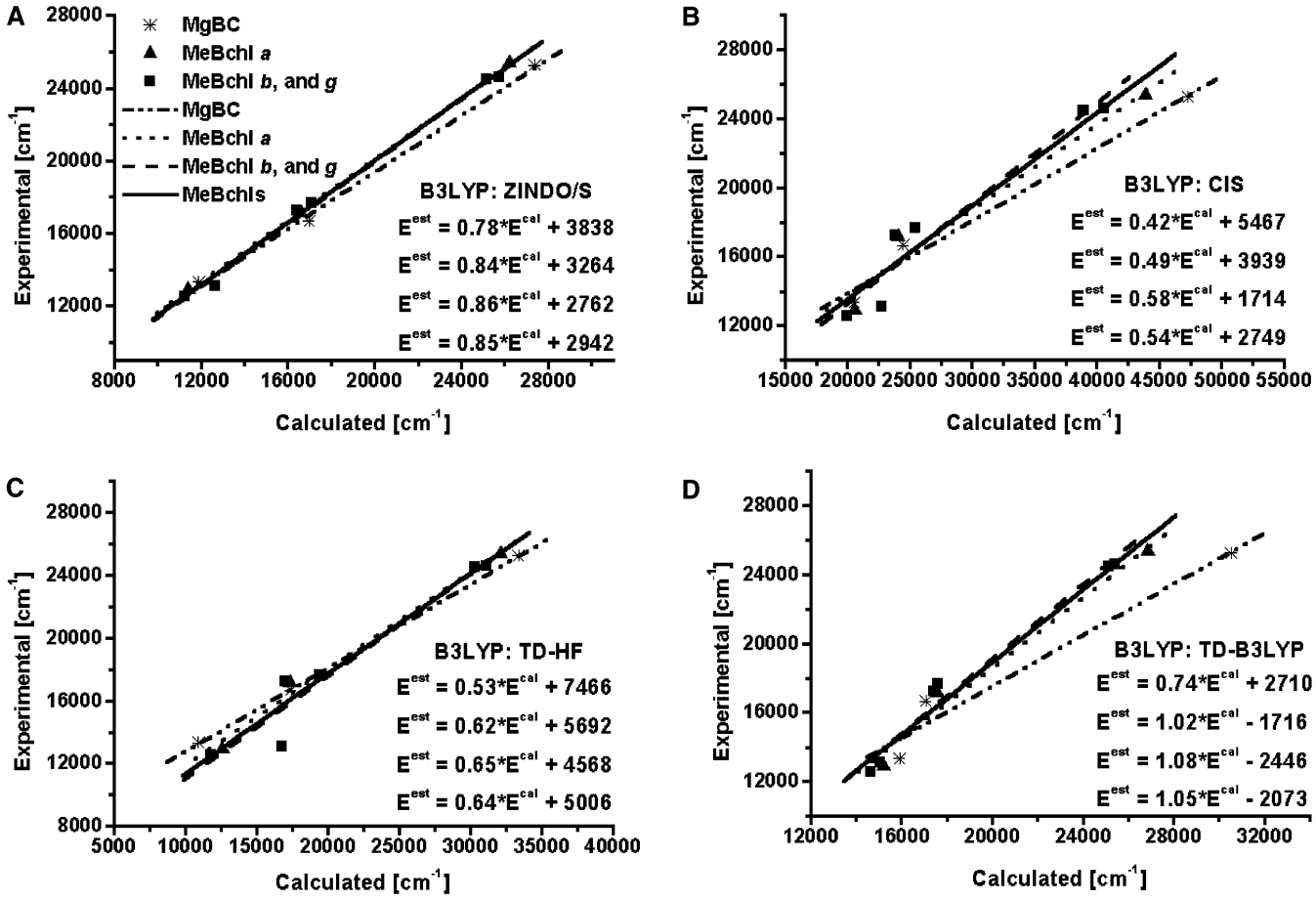

Figure 4. Correlations of the calculated and experimental solution transition energies of B3LYP/6-31G* optimized five coordinated methyl bacteriochlorophylls. Equations in the insert from top to bottom refer to Mg−BC, MeBchl *a*, MeBchl *b* and *g*, all MeBchls, respectively.

TABLE 3: Most Important Atomic Charges (Mulliken Population Analysis) of Mg−Bacteriochlorin and Methyl Bacteriochlorophyllides[a]

atom	Mg−BC	MeBchl *a*	MeBchl *b*	MeBchl *g*	MeBchl *h*
Mg	0.85 (0.83)	0.85 (0.83)	0.86 (0.84)	0.86 (0.84)	0.85 (0.83)
	1.21 (1.28)	1.22 (1.28)	1.22 (1.29)	1.22 (1.29)	1.22 (1.28)
NA	−0.72 (−0.71)	−0.75 (−0.74)	−0.75 (−0.74)	−0.76 (−0.75)	−0.75 (−0.75)
	−0.98 (−0.96)	−1.01 (−1.00)	−1.01 (−1.00)	−1.01 (−1.00)	−1.01 (−1.00)
NB	−0.62 (−0.61)	−0.64 (−0.62)	−0.68 (−0.66)	−0.68 (−0.66)	−0.64 (−0.62)
	−0.83 (−0.80)	−0.84 (−0.81)	−0.87 (−0.84)	−0.87 (−0.84)	−0.84 (−0.82)
NC	−0.72 (−0.70)	−0.77 (−0.75)	−0.77 (−0.75)	−0.77 (−0.75)	−0.77 (−0.74)
	−0.93 (−0.91)	−0.98 (−0.96)	−0.98 (−0.96)	−0.98 (−0.96)	−0.98 (−0.95)
ND	−0.62 (−0.61)	−0.65 (−0.64)	−0.65 (−0.64)	−0.65 (−0.64)	−0.65 (−0.64)
	−0.83 (−0.80)	−0.85 (−0.83)	−0.85 (−0.83)	−0.85 (−0.83)	−0.85 (−0.83)
$O13^1$		−0.48 (−0.49)	−0.48 (−0.48)	−0.48 (−0.49)	−0.48 (−0.49)
		−0.59 (−0.59)	−0.58 (−0.59)	−0.59 (−0.59)	−0.59 (−0.59)
$=O13^2$		−0.49 (−0.49)	−0.49 (−0.49)	−0.49 (−0.50)	−0.49 (−0.50)
		−0.59 (−0.59)	−0.59 (−0.59)	−0.59 (−0.59)	−0.59 (−0.59)
$O13^2$		−0.45 (−0.44)	−0.45 (−0.44)	−0.44 (−0.44)	−0.44 (−0.44)
		−0.60 (−0.60)	−0.60 (−0.60)	−0.60 (−0.60)	−0.60 (−0.60)
=OR17		−0.47 (−0.47)	−0.47 (−0.47)	−0.50 (−0.48)	−0.47 (−0.47)
		−0.56 (−0.56)	−0.56 (−0.56)	−0.56 (−0.56)	−0.56 (−0.56)
OR17		−0.45 (−0.45)	−0.45 (−0.45)	−0.45 (−0.45)	−0.45 (−0.45)
		−0.61 (−0.61)	−0.61 (−0.61)	−0.61 (−0.61)	−0.61 (−0.61)
OR3		−0.47 (−0.48)	−0.47 (−0.48)		
		−0.51 (−0.52)	−0.50 (−0.52)		

[a] Top row B3LYP/6-31G* atomic charge, bottom row HF/6-31G* atomic charge. Values in parenthesis are for 1:1 complexes. Total charge in the columns does not add to zero as most of the atomic charges of the pigments are not shown.

surprising since experimental transition energies of bacteriochlorophyll like molecules have been reported to be much higher in supersonic expansion than in the gas, liquid, or solid phases (for example the Q_y transition energy of MgTPP in supersonic expansion is about 460, 630, and 790 cm^{-1} larger than it in gas phase, benzene solution, or ethanol glass, respectively).[123−125] It is then to be expected that even for the 1:1 solvent complexes calculated values are higher than the experimental solution transition energies. The ZINDO/S CIS and TD-HF methods with B3LYP/6-31G* optimized structures both seem to give results

TABLE 4: Estimated and Experimental Absorption Band Positions (nm) and Oscillator Strengths (*f*) of Four Coordinated (vacuum) Mg−BC and Methyl Bacteriochlorophylls Optimized by HF and B3LYP Methods

molecule	Q_y [nm] (*f*)	Q_x [nm] (*f*)	Soret [nm] (*f*)
Mg−BC B3LYP	767 (0.7)	585 (0.0)	**397** (2.4)
	714 (0.9)	631 (0.0)	489, 479, 433, 423, **394** (4.3)
	763 (0.0)	588 (0.0)	**398** (0.1)
	741 (0.1)	608 (0.0)	452, 430, **395** (0.9)
Mg−BC HF	774 (0.4)	579 (0.0)	**399** (1.2)
	682 (0.6)	655 (0.1)	460, 436, **395** (2.5)
	690 (0.1)	649 (0.4)	**394** (1.6)
	763 (0.1)	588 (0.0)	480, **398** (0.7)
exp.[b]	750	600	396
MeBchl *a* B3LYP	782 (0.9)	575 (0.0)	422, 410, 403, **395** (1.2)
	717 (1.1)	628 (0.1)	442, 429, 421, 413, **391** (1.7)
	768 (0.3)	587 (0.1)	**393** (1.1)
	747 (0.2)	605 (0.1)	457, 441, 423, 401, **392** (0.3)
MeBchl *a* HF	777 (0.4)	579 (0.1)	430, 410, **395** (1.0)
	681 (0.3)	654 (0.6)	415, **392** (1.9)
	745 (0.2)	606 (0.6)	**391** (1.4)
	764 (0.2)	591 (0.1)	492, 477, 411, 406, **393** (0.3)
exp.[c]	773	583	394
MeBchl *b* B3LYP	798 (0.8)	579 (0.0)	423, 416, **412** (0.6)
	744 (1.0)	639 (0.0)	438, 419, 412, **406** (1.3)
	829 (0.3)	623 (0.0)	**411** (1.4)
	770 (0.2)	602 (0.1)	449, 439, 437, **411** (0.4)
MeBchl *b* HF	774 (0.4)	590 (0.0)	425, 420, **406** (1.5)
	700 (0.3)	656 (0.5)	**404** (0.6)
	775 (0.1)	602 (0.6)	**407** (2.0)
	785 (0.2)	582 (0.1)	475, 460, **410** (0.3)
exp.[d]	796	579	408
MeBchl *g* B3LYP	757 (0.7)	568 (0.0)	420, **402** (1.3), 396, 392, 383, 376, 371, **358** (0.5)
	684 (0.9)	609 (0.0)	431, 427, 410, **400** (2.8), 382, 361, 358, **344** (2.2)
	664 (0.4)	575 (0.1)	**403** (1.7), 386, 352, **337** (0.9)
	747 (0.2)	577 (0.0)	457, 438, 415, **398** (0.7), 381, 373, **349** (0.7)
MeBchl *g* HF	745 (0.4)	585 (0.0)	440, **402** (1.6), 387, **375** (0.4)
	673 (0.1)	630 (0.6)	**404** (1.0), **395** (0.7)
	748 (0.1)	573 (0.7)	**403** (2.0), **342** (0.5)
	763 (0.2)	572 (0.1)	465, 451, 407, **403** (0.6), 378, 368, **348** (0.6)
exp.[c]	763	566	406, 366
MeBchl *h* B3LYP	756 (0.7)	566 (0.0)	420, **399** (0.3)
	667 (1.0)	601 (0.1)	438, 434, 420, **398** (0.9)
	630 (0.4)	548 (0.1)	389, **384** (1.5)
	730 (0.2)	578 (0.1)	464, 446, 410, **378** (0.6)
MeBchl *h* HF	731 (0.4)	568 (0.1)	430, **388** (0.9)
	649 (0.2)	618 (0.6)	413, 402, 383, **375** (1.9)
	709 (0.2)	569 (0.7)	**386** (1.3)
	729 (0.2)	567 (0.1)	475, 461, 407, **392** (0.6)
exp.			

[a] The four rows of transition energies from top to bottom refer to ZINDO/S CIS (40,40), ab initio CIS (5,5), TD-HF, and TD-B3LYP results, respectively. The main Soret transition is printed in bold, transitions below the Soret band are considered as dark states. [b] Reference 134. [c] In acetone ref 49. [d] In ethyl ether ref 49.

that compare nicely with solution values (except TD-HF for Soret energy). Finally, these methods may underestimate the true transition energies. The ZINDO/S CIS method is parametrized by using liquid and gas-phase parameters, which must be, at least partially, the reason for good correlations with the experimental solution values. The TD-HF and ab initio CIS methods produce much larger separation of the Q_x and Soret states than is obtained with the other methods, for both HF and B3LYP geometries (see Figure 3). The TD-HF and ab initio CIS methods seem consistently to overestimate the transition energies, especially the Soret transition energies (Figure 3). The largest overestimation of the experimental transition energies is obtained for HF geometries with configuration interaction for single excitations.

3.3.2. Estimated Transition Energies. In Tables 4 and 5, estimated transition energies are shown for monomeric MeBchls and Mg−BC and their 1:1 acetone complexes, respectively. Transition energies of MeBchl *h* were estimated by using linear equations obtained for MeBchl *a*. The linear correlations between the calculated and experimental transition energies are shown for B3LYP optimized 1:1 complexes in Figure 4. In general, the correlations with the experimental solution transition energies were better for the 1:1 complexes than for the vacuum pigments. The HF and B3LYP geometries with TD-B3LYP transition energies gave closest to ideal correlations, with nearly slope one and almost zero intercept (within the accuracy of calculations) and correlation coefficients better than 0.99 (Figure 4D). These methods are computationally very demanding and far too expensive to be practical to be used in the study of porphyrines in protein environments. HF geometries with TD-HF transition energies gave correlations with nearly unity slope, but the intercept was far below zero. The best correlation coefficients between the calculated and experimental transition energies were obtained for B3LYP geometries with ZINDO/S transition energies (Figure 4A). This approach seems to us as a good compromise for work with photosynthetic protein complexes. Yet, the computationally much less demanding PM5 method for geometry optimization with ZINDO/S for calculation

TABLE 5: Estimated and Experimental Absorption Bands Positions (nm) and Oscillator Strengths (*f*) of Five Coordinated (1:1 Acetone Complexes) Mg−BC and Methyl Bacteriochlorophylls Optimized by HF and B3LYP Methods[a]

molecule	Q_y [nm] (*f*)	Q_x [nm] (*f*)	Soret [nm] (*f*)
Mg−BC B3LYP	761 (0.6)	590 (0.0)	569, **397** (2.0)
	714 (0.9)	631 (0.0)	489, 479, 433, 423, **394** (4.3)
	753 (0.2)	597 (0.0)	**396** (1.2)
	689 (0.0)	650 (0.1)	579, 538, 447, 427, **394** (0.9)
Mg−BC HF	754 (0.4)	596 (0.0)	552, **396** (1.2)
	677 (0.1)	659 (0.8)	395, **400** (0.4)
	729 (0.1)	618 (0.4)	**394** (1.5)
	704 (0.1)	639 (0.0)	565, 512, 462, 405, **394** (0.5)
exp.[b]	750	600	396
MeBchl *a* B3LYP	775 (0.8)	581 (0.1)	509, 417, 402, **394** (1.0)
	710 (1.0)	633 (0.1)	426, 408, 404, **391** (1.3)
	742 (0.3)	609 (0.1)	**391** (1.0)
	728 (0.2)	620 (0.1)	607, 500, 442, 427, 424, 401, **391** (0.2)
MeBchl *a* HF	750 (0.4)	602 (0.1)	499, 434, 412, **392** (0.8)
	706 (0.2)	636 (0.7)	**391** (1.7)
	780 (0.2)	577 (0.7)	**395** (1.2)
	732 (0.2)	616 (0.0)	598, 506, 466, 461, 408, 398, **391** (0.3)
exp.[c]	773	583	394
MeBchl *b* B3LYP	797 (0.7)	592 (0.0)	510, 417, **410** (0.9)
	752 (1.0)	643 (0.0)	**412** (0.9)
	816 (0.3)	639 (0.0)	**411** (1.3)
	748 (0.2)	611 (0.0)	594, 477, 424, 423, **405** (0.4)
MeBchl *b* HF	759 (0.4)	616 (0.1)	509, 437, 418, **406** (1.4)
	727 (0.1)	647 (0.6)	**405** (2.2)
	812 (0.1)	584 (0.7)	**413** (1.8)
	749 (0.1)	613 (0.0)	589, 488, 448, 443, **408** (0.4)
exp.[d]	796	579	408
MeBchl *g* B3LYP	738 (0.6)	574 (0.0)	502, **401** (1.5), 395, 389, 375, 365, 364, 354, **339** (0.6)
	671 (0.9)	607 (0.0)	416, **396** (2.6), 380, 362, 354, 341, 338, **329** (1.3)
	645 (0.4)	581 (0.0)	**403** (1.5), 386, 348, **326** (1.1)
	725 (0.2)	603 (0.0)	575, 467, 445, 409, **400** (0.2), **387** (0.5)
MeBchl *g* HF	712 (0.4)	601 (0.1)	504, 438, **400** (1.4), 380, **369** (0.6)
	695 (0.1)	606 (0.7)	**401** (1.7), **365** (1.1)
	764 (0.1)	544 (0.8)	**406** (1.8), 345, 313, 305, **286** (1.4)
	710 (0.1)	612 (0.0)	564, 486, 432, 428, **397** (0.3), **389** (0.5)
exp.[c]	763	566	406, 366
MeBchl *h* B3LYP	720 (0.7)	564 (0.0)	512, 398, **396** (0.4)
	644 (1.0)	601 (0.1)	437, 406, **394** (1.8)
	601 (0.4)	558 (0.1)	389, **376** (1.5)
	713 (0.2)	622 (0.0)	584, 494, 458, 429, 408, **376** (0.6)
MeBchl *h* HF	702 (0.4)	587 (0.1)	496, 420, **386** (0.8)
	683 (0.2)	604 (0.8)	406, **373** (1.6)
	738 (0.2)	543 (0.8)	**392** (1.0)
	704 (0.1)	608 (0.0)	574, 501, 449, 445, 405, **385** (0.5)
exp.			

[a] The four rows from top to bottom refer to ZINDO/S CIS (45,45), ab initio CIS (6,6), TD-HF, and TD-B3LYP results, respectively. The main Soret transition is printed in bold, transitions below the Soret band are considered as dark states. [b] Reference 134. [c] In acetone ref 49. [d] In ethyl ether ref 49.

of transition energies has been shown to produce results that are not much inferior to those obtained from the B3LYP−ZINDO/S approach.[57] The least ideal correlations were obtained for the B3LYP geometries with CIS transition energies (Figure 4B). From the above discussion it is clear that the computational methods used are more or less inaccurate in prediction of transition energies in bacteriochlorins as almost every method produced its characteristic fitting parameters, in some cases very far from ideal behavior.

To study the effect of rotation of the acetyl group of Bchl *a* on transition energies, 1:1 complex structure was used with B3LYP/6-31G and ZINDO/S CIS methods. The value of the dihedral angle C2−C3−CR3−CR3′ was varied from −40 to +40° in the range reported in various X-ray structure determinations.[4,7,8,96−99,126] Calculations suggest that the fully optimized structure (dihedral angle almost 0°) has the lowest Q_y, Q_x, and Soret transition energies and that the energies increase as the dihedral angle C2−C3−CR3−CR3′ increases. The Soret energy seems to be more sensitive to the conformation change than the Q_y and Q_x energies. Energy differences between structures with dihedral angles of 0° and ±40° are about 320, 160, and 450 cm^{-1} for Q_y, Q_x, and Soret energies, respectively. The calculations show that the off-plane conformation of acetyl group has an effect on transition energies as has been previously suggested.[11]

The TD-B3LYP and the ZINDO/S methods gave the clearest evidence on the presence of dark electronic states (i.e., states that are not optically allowed in ground state absorption) below the main Soret transition in Bchls (see Figure 3, thin light gray lines, Tables 4 and 5). The number of dark states is higher in the 1:1 complexes than in vacuum pigments. It may be asked, are these dark states real or simply states generated by the computational method? Our previous ZINDO/S CIS study for the PM5 optimized Chl and Bchl molecules indicated existence of dark electronic states.[57] Also time dependent density functional and multireference configuration interaction calculations on Chl *a* and Bchl *b* molecules produce such states.[67,127,128] Hence computations give evidence of the existence of dark states

with energies depending on the geometry and electron density of the porphyrin skeleton.[57] The Soret region of porphyrines contains a number of close lying electronic states. Some of these states could be sensitive to 1:1 solvent interaction (or protein interaction). Such an interaction may result in mixing of states and levels with low oscillation strengths appearing below the main Soret transition. The number of dark electronic states will depend on the conformation and/or environment of the chromophore. Actually, ZINDO/S CIS calculations for the B3LYP 1:1 MeBchl *a* and acetone complex structures with different acetyl group conformation (dihedral angle C2−C3−CR3−CR3′ was changed from −40 to +40°) suggest that conformation of the acetyl group has also an effect on the number of dark states below the main Soret state.

In the experimental absorption spectra of Chls or Bchls, the existence of transitions with low oscillator strengths below the Soret region have not been reported. Yet examination of the spectra indicates that there is nonzero absorption in all spectra before the main Soret absorptions build up. Electronic states with low absorption strength can serve as intermediate states in the down hill energy transfer in photosynthetic light harvesting antenna. Particularly interesting is the role of these states in carotenoid to Chl and Bchl energy transfer as they are positioned in the region of carotenoid absorption and some of these states could be very close to excited carotenoid energy levels. Our ZINDO/S CIS (45,45) calculations for B800 Bchl *a* of light harvesting antenna two (LH2) complexes of purple bacteria with its nearest amino acids (closer than 8 Å from the bacteriochlorin plane) included in the calculation give from three to five dark states below the main Soret transitions. The Q_x and Soret transition energies are also red shifted by a few hundred wavenumbers with respect to the vacuum B800 Bchl *a* transitions. Similar results have been reported in a recent TD-DFT study for B800 Bchl *a*'s.[42] There are a couple of experimental findings that may be related to dark states. The femtosecond infrared study of monomeric Bchl *a* in acetone solution gives evidence of existence of an electronic state(s) corresponding to one-photon transition(s) around 470 nm, in the region where our calculations predict dark transitions to occur.[129] A dark state could have been observed also in carotenoids. To explain experimental kinetic results from carotenoids to Bchls existence of intermediate S* carotenoid state below the S2 state has been suggested.[130]

It is pointed out that the environment modifies the geometry, the charge (electron) distribution, and hence the transition energies of a pigment. In particular, the energy difference between Q_y and Q_x states in the MeBchls studied is smaller in the 1:1 complex than in the monomer (from 4 or 5 coordinated structures) as a result of acetone coordination that perturbs the electron density around the Mg atom. This observation suggests that the model system for a pigment in a protein environment has to include at least the nearest surrounding amino acids and other nearby molecules that interact with the chromophore to be able to describe electron density (wave functions) correctly.[35,41,42,131]

The results presented in Tables 4 and 5 show how the various methods used predict the electronic transition energies of the MeBchls studied. Best transition energies are obtained by using ZINDO/S CIS or TD-B3LYP methods with B3LYP geometries. Most important spectroscopic features of the Bchls are reproduced reasonably well. There are, however, three points to be made on calculated oscillator strengths (calculated oscillator strengths are compared to the absorbance values obtained from experimental spectrum, not shown). First, it seems that the TD methods produce oscillation strengths quite poorly. Second, ab initio CIS (5,5) or (6,6) and TD-HF methods for HF optimized structures give too strong oscillation strengths for the Q_x transitions. Finally, the ZINDO/CIS method for B3LYP optimized structures seem to underestimate the oscillation strengths of the Q_x transitions. Increasing the size of the basis set from 6-31G* to 6-311G** in the calculations seems not to have an effect on the calculated oscillation strengths. This means that the methods used are not well enough developed for prediction of the electronic transition dipole moments correctly.

The simple SCRF method was used to study bulk solvent effects on transition energies. In the B3LYP optimized structures, Q_y transition energies were blue shifted a few hundreds of wavenumbers, whereas the Q_x and Soret energies were not much shifted from vacuum numbers. For the HF optimized structures, Q_y transition energies were blue shifted more than 1500 cm^{-1} and Q_x and Soret energies about 500 cm^{-1}. Over all, the SCRF method produces quite good correlations for transition energies for the B3LYP optimized structures (vacuum and 1:1 complexes), and the HF optimized structures produced poorer correlations. The inclusion of the bulk solvent effect in the calculation resulted in few new dark states below the main Soret transition. Changing the solvent parameters of the SCRF calculation showed that energies of states whose dipole moments differ considerably from the ground state dipole moment are sensitive to the bulk solvent environment. Thus, not only structural changes but also the surrounding induces electron density redistributions making additional dark electronic states to appear. A similar result was obtained by including the protein environment in calculations of the transition energies for the B800 Bchl *a*. We think that this is valid also in general, where a molecule in a different environment (solvent, protein, etc.) might have a number of dark electronic states below a main transition.

There is one important difference between the present calculations and our previous semiempirical PM3 studies of bacteriochlorophylls.[50] In the present calculations, the Q_x transition energies of Bchls are clearly better predicted than in the ZINDO/S−PM3 study.[50] As discussed above, this can be traced back to a wrong positioning of the Mg atom in the bacteriochlorin due to inadequate parametrization of the PM3 method. Ab initio and density functional methods put the Mg atom nearly in the center of the bacteriochlorin ring as observed in many crystal structures and give more accurate Q_x transition energies for Bchls. The semiempirical PM5 method also works well in this respect.[57] The HF and B3LYP optimized Chl *a* give the Q_x transition energies also better than the PM3 optimized Chl *a*.[132] It seems that transition energies of bacteriochlorophylls and chlorophylls that involve magnesium orbitals are dependent on the position of the Mg atom with respect to the porphyrin skeleton, especially the Q_x state which seems to have large Mg character.

Differences in HF and B3LYP bond lengths of the bacteriochlorin ring resulted in large differences in calculated electronic transition energies (Figure 3). The observation means that calculations based on X-ray structures with different experimental resolution may give very different results! To demonstrate this, a Bchl *a*1 of the Fenna−Matthews−Olson (FMO) protein of *Prosthecochloris aestuarii* was used as a model system.[133] Coordinates of the Bchl *a*1 molecule were obtained from three different X-ray structure determinations of the complex. In the calculations, hydrogen atoms were added to the structures, and their positions were optimized by using the PM3 method and keeping the non-hydrogen atoms fixed to their

X-ray coordinates.[7,133−135] The bond length differences of the three structure determinations displayed in Table 2 are large enough to introduce significant shifts of the calculated transition energies. The ZINDO/S CIS (40,40) calculated Q_y transition energy difference is as large as 100 nm between the low and high resolution determinations. Linear correlations discussed above will help in getting around with this problem.

4. Conclusions

The results of this paper show that the density functional B3LYP/6-31G* method suits for prediction of structures of Mg−BC, MeBchls, and their 1:1 acetone complexes. Due to differences of the HF and B3LYP geometries, the calculated electronic transition from HF geometries were systematically higher (and clearly higher than the experimental transition energies) than the corresponding values obtained from B3LYP geometries. Transition energies calculated for a chromophore in a protein site by using experimental X-ray coordinates from determinations of different accuracy showed also large variations. To allow comparison of transition energies of chromophores in different environments and from different computational approaches, use of linear regression with experimental energies proved to be useful, as suggested by Petke long ago. It was shown that the size of the model system chosen for calculations is critical in terms of reliability of the results to be obtained. The environment of the pigment does not only modify the geometry of the chromophore but it also modifies the electron density, which is further reflected in the positions of the energy levels. Complexation of the pigments induce dark electronic states below the main Soret transition. Such dark states might have an important role in energy transfer in photosynthetic protein complexes, in particular from carotenoid to Chl or Bchl energy transfer.

Acknowledgment. The authors acknowledge the grant from Academy of Finland (Contract No. 50670). Generous computing resources provided by Prof. Jussi Timonen of the Department of Physics of the University of Jyväskylä are greatly appreciated.

Supporting Information Available: Calculated heavy atom distances (Table 1S), calculated transition energies for vacuum structures (Table 2S), calculated transition energies for 1:1 complex structures (Table 3S), and linear regressions for Mg−BC and MeBchls vacuum and 1:1 acetone complex structures (Table 4S). This material is available free of charge via the Internet at http://pubs.acs.org.

References and Notes

(1) van Grondelle, R.; Dekker, J. P.; Gillbro, T.; Sundström, V. *Biochim. Biophys. Acta* **1994**, *1187*, 1.
(2) Friesner, R. A.; Won, Y. *Biochim. Biophys. Acta* **1989**, *977*, 99.
(3) Deisenhofer, J.; Epp, O.; Miki, K.; Huber, R.; Michel, H. *Nature* **1985**, *318*, 618.
(4) McDermott, G.; Prince, S. M.; Freer, A. A.; Hawthornthwaite-Lawless, A. M.; Papiz, M. Z.; Cogdell, R. J.; Isaacs, N. W. *Nature* **1995**, *374*, 517.
(5) Hu, X.; Xu, D.; Hamer, K.; Schulten, K.; Koepke, J.; Michel, H. *Protein Sci.* **1995**, *4*, 1670.
(6) Freer, A.; Prince, S.; Sauer, K.; Papiz, M.; Hawthornthwaite-Lawless, A.; McDermott, G.; Cogdell, R.; Isaacs, N. W. *Structure* **1996**, *4*, 449.
(7) Tronrud, D. E.; Schmid, M. F.; Matthews, B. W. *J. Mol. Biol.* **1986**, *188*, 443.
(8) Deisenhofer, J.; Michel, H. *EMBO J.* **1989**, *8*, 2149.
(9) Roszak, A. W.; Howard, T. D.; Southall, J.; Gardiner, A. T.; Law, C. J.; Isaacs, N. W.; Cogdell, R. J. *Science* **2003**, *302*, 1969.
(10) Warshel, A.; Parson, W. W. *J. Am. Chem. Soc.* **1987**, *109*, 6143.
(11) Parson, W. W.; Warshel, A. *J. Am. Chem. Soc.* **1987**, *109*, 6152.
(12) Scherer, P. O. J.; Fischer, S. F. *Chem. Phys.* **1989**, *131*, 115.
(13) Thompson, M. A.; Zerner, M. C. *J. Am. Chem. Soc.* **1991**, *113*, 8210.
(14) Scherer, P. O. J.; Scharnagl, C.; Fischer, S. F. *Chem. Phys.* **1995**, *197*, 333.
(15) Hutter, M. C.; Hughes, J. M.; Reimers, J. R.; Hush, N. S. *J. Phys. Chem. B* **1999**, *103*, 4906.
(16) Nakatsuji, H.; Hasegawa, J.; Ohkawa, K. *Chem. Phys. Lett.* **1998**, *296*, 499.
(17) Ivashin, N.; Källebring, B.; Larsson, S.; Hansson, Ö. *J. Phys. Chem. B* **1998**, *102*, 5017.
(18) Cory, M. G.; Zerner, M. C.; Hu, X.; Schulten, K. *J. Phys. Chem. B* **1998**, *102*, 7640.
(19) Hasegawa, J.; Nakatsuji, H. *J. Phys. Chem. B* **1998**, *102*, 10420.
(20) Palaniappan, V.; Martin, P. C.; Chynwat, V.; Frank, H. A.; Bocian, D. F. *J. Am. Chem. Soc.* **1993**, *115*, 12035.
(21) Creighton, S.; Hwang, J.-K.; Warshel, A.; Parson, W. W.; Norris, J. *Biochemistry* **1988**, *27*, 774.
(22) Ivashin, N.; Larsson, S. *J. Phys. Chem. B* **2002**, *106*, 3996.
(23) Scherer, P. O. J.; Fischer, S. F. *J. Phys. Chem.* **1989**, *93*, 1633.
(24) Hanson, L. K.; Fajer, J.; Thompson, M. A.; Zerner, M. C. *J. Am. Chem. Soc.* **1987**, *109*, 4728.
(25) Thompson, M. A.; Zerner, M. C.; Fajer, J. *J. Phys. Chem.* **1990**, *94*, 3820.
(26) Källebring, B.; Larsson, S. *Chem. Phys. Lett.* **1987**, *138*, 76.
(27) Sakuma, T.; Takada, T.; Kashiwagi, H.; Nakamura, H. *Int. J. Quantum Chem. Quantum Biol. Symp.* **1990**, *17*, 93.
(28) Gudowska-Nowak, E.; Newton, M. D.; Fajer, J. *J. Phys. Chem.* **1990**, *94*, 5795.
(29) Thompson, M. A.; Fajer, J. *J. Phys. Chem.* **1992**, *96*, 2933.
(30) Thompson, M. A.; Schenter, G. K. *J. Phys. Chem.* **1995**, *99*, 6374.
(31) Cory, M. G.; Zerner, M. C. *J. Am. Chem. Soc.* **1996**, *118*, 4148.
(32) Sakuma, T.; Kashiwagi, H.; Takada, T.; Nakamura, H. *Int. J. Quantum Chem.* **1997**, *61*, 137.
(33) Krueger, B. P.; Scholes, G. D.; Fleming, G. R. *J. Phys. Chem. B* **1998**, *102*, 5378.
(34) Hasegawa, J.; Ohkawa, K.; Nakatsuji, H. *J. Phys. Chem. B* **1998**, *102*, 10410.
(35) Linnanto, J.; Korppi-Tommola, J. E. I.; Helenius, V. M. *J. Phys. Chem. B* **1999**, *103*, 8739.
(36) Scholes, G. D.; Gould, I. R.; Cogdell, R. J.; Fleming, G. R. *J. Phys. Chem. B* **1999**, *103*, 2543.
(37) Alden, R. G.; Johnson, E.; Nagarajan, V.; Parson, W. W.; Law, C. J.; Cogdell, R. G. *J. Phys. Chem. B* **1997**, *101*, 4667.
(38) Tretiak, S.; Middleton, C.; Chernyak, V.; Mukamel, S. *J. Phys. Chem. B* **2000**, *104*, 4519.
(39) Tretiak, S.; Middleton, C.; Chernyak, V.; Mukamel, S. *J. Phys. Chem. B* **2000**, *104*, 9540.
(40) Ihalainen, J. A.; Linnanto, J.; Myllyperkiö, P.; van Stokkum, I. H. M.; Ücker, B.; Scheer, H.; Korppi-Tommola, J. E. I. *J. Phys. Chem. B* **2001**, *105*, 9849.
(41) Linnanto, J.; Korppi-Tommola, J. E. I. *Phys. Chem. Chem. Phys.* **2002**, *4*, 3453.
(42) He, Z.; Sundström, V.; Pullerits, T. *J. Phys. Chem. B* **2002**, *106*, 11606.
(43) Scholes, G. D.; Fleming, G. R. *J. Phys. Chem. B* **2000**, *104*, 1854.
(44) Linnanto, J. M.; Korppi-Tommola, J. E. I. *J. Chin. Chem. Soc.* **2000**, *47*, 657.
(45) Scherer, P. O. J.; Fischer, S. F. *Chem. Phys. Lett.* **1987**, *141*, 179.
(46) Blomberg, M. R. A.; Siegbahn, P. E. M.; Babcock, G. T. *J. Am. Chem. Soc.* **1998**, *120*, 8812.
(47) Wang, Y.; Hu, X. *J. Chem. Phys.* **2002**, *117*, 1.
(48) Scherer, P. O. J.; Fischer, S. F. In *The reaction center of photosynthetic bacteria: Structure and dynamics*; Springer-Verlag: Heidelberg, 1996; pp 89−104.
(49) Thompson, M. A.; Zerner, M. C.; Fajer, J. *J. Phys. Chem.* **1991**, *95*, 5693.
(50) Linnanto, J.; Korppi-Tommola, J. *J. Phys. Chem. A* **2001**, *105*, 3855.
(51) Hanson, L. K. *Photochem. Photobiol.* **1988**, *47*, 903.
(52) Philipson, K. D.; Tsai, S. C.; Sauer, K. *J. Phys. Chem.* **1971**, *75*, 1440.
(53) Zhang, L. Y.; Friesner, R. A. *J. Phys. Chem.* **1995**, *99*, 16479.
(54) Davis, M. S.; Forman, A.; Hanson, L. K.; Thornber, J. P.; Fajer, J. *J. Phys. Chem.* **1979**, *83*, 3325.
(55) Barkigia, K. M.; Chantranupong, L.; Smith, K. M.; Fajer, J. *J. Am. Chem. Soc.* **1988**, *110*, 7566.
(56) Facelli, J. C. *J. Phys. Chem. B* **1998**, *102*, 2111.
(57) Linnanto, J.; Korppi-Tommola, J. *J. Comput. Chem.* **2004**, *25*, 123.
(58) Petke, J. D.; Maggiora, G. M.; Shipman, L. L.; Christoffersen, R. E. *Photochem. Photobiol.* **1981**, *33*, 663.
(59) Petke, J. D.; Maggiora, G. M.; Shipman, L. L.; Christoffersen, R. E. *Photochem. Photobiol.* **1980**, *32*, 399.

(60) Petke, J. D.; Maggiora, G. M.; Shipman, L. L.; Christoffersen, R. E. *Photochem. Photobiol.* **1980**, *31*, 243.
(61) Donohoe, R. J.; Frank, H. A.; Bocian, D. F. *Photochem. Photobiol.* **1988**, *48*, 531.
(62) Otten, H. A. *Photochem. Photobiol.* **1971**, *14*, 589.
(63) O'Malley, P. J.; Collins, S. J. *J. Am. Chem. Soc.* **2001**, *123*, 11042.
(64) Sinnecker, S.; Koch, W.; Lubitz, W. *Phys. Chem. Chem. Phys.* **2000**, *2*, 4772.
(65) Mercer, I. P.; Gould, I. R.; Klug, D. R. *J. Phys. Chem. B* **1999**, *103*, 7720.
(66) Yerushalmi, R.; Noy, D.; Baldridge, K. K.; Scherz, A. *J. Am. Chem. Soc.* **2002**, *124*, 8406.
(67) Sundholm, D. *Phys. Chem. Chem. Phys.* **2003**, *5*, 4265.
(68) Frisch, M. J.; Trucks, G. W.; Schlegel, H. B.; Scuseria, G. E.; Robb, M. A.; Cheeseman, J. R.; Zakrzewski, V. G.; Montgomery, J. A., Jr.; Stratmann, R. E.; Burant, J. C.; Dapprich, S.; Millam, J. M.; Daniels, A. D.; Kudin, K. N.; Strain, M. C.; Farkas, O.; Tomasi, J.; Barone, V.; Cossi, M.; Cammi, R.; Mennucci, B.; Pomelli, C.; Adamo, C.; Clifford, S.; Ochterski, J.; Petersson, G. A.; Ayala, P. Y.; Cui, Q.; Morokuma, K.; Malick, D. K.; Rabuck, A. D.; Raghavachari, K.; Foresman, J. B.; Cioslowski, J.; Ortiz, J. V.; Stefanov, B. B.; Liu, G.; Liashenko, A.; Piskorz, P.; Komaromi, I.; Gomperts, R.; Martin, R. L.; Fox, D. J.; Keith, T.; Al-Laham, M. A.; Peng, C. Y.; Nanayakkara, A.; Gonzalez, C.; Challacombe, M.; Gill, P. M. W.; Johnson, B. G.; Chen, W.; Wong, M. W.; Andres, J. L.; Head-Gordon, M.; Replogle, E. S.; Pople, J. A. *Gaussian 98*, revision A.6; Gaussian, Inc.: Pittsburgh, PA, 1998.
(69) Ridley, J.; Zerner, M. *Theor. Chim. Acta (Berlin)* **1973**, *32*, 111.
(70) Karlsson, G.; Zerner, M. C. *Int. J. Quantum Chem.* **1973**, *7*, 35.
(71) Ridley, J. E.; Zerner, M. C. *Theor. Chim. Acta (Berlin)* **1976**, *42*, 223.
(72) Zerner, M. C.; Loew, G. H.; Kirchner, R. F.; Mueller-Westerhoff, U. T. *J. Am. Chem. Soc.* **1980**, *102*, 589.
(73) Karelson, M. M.; Zerner, M. C. *J. Phys. Chem.* **1992**, *96*, 6949.
(74) *CRC Handbook of chemistry and physics*, 74 ed.; CRC Press: Boca Raton, FL, 1994.
(75) Jordan, P.; Fromme, P.; Witt, H. T.; Klukas, O.; Saenger, W.; Kraub, N. *Nature* **2001**, *411*, 909.
(76) Kühlbrandt, W.; Wang, D. N.; Fujiyoshi, Y. *Nature* **1994**, *367*, 614.
(77) Bhyrappa, P.; Wilson, S. R.; Suslick, K. S. *J. Am. Chem. Soc.* **1997**, *119*, 8492.
(78) Hofmann, E.; Wrench, P. M.; Sharples, F. P.; Hiller, R. G.; Welte, W.; Diederichs, K. *Science* **1996**, *272*, 1788.
(79) Balch, A. L. *Coord. Chem. Rev.* **2000**, *200*−*202*, 349.
(80) Serlin, R.; Chow, H.-C.; Strouse, C. E. *J. Am. Chem. Soc.* **1975**, *97*, 7237.
(81) Chow, H.-C.; Serlin, R.; Strouse, C. E. *J. Am. Chem. Soc.* **1975**, *97*, 7230.
(82) Barkigia, K. M.; Miura, M.; Thompson, M. A.; Fajer, J. *Inorg. Chem.* **1991**, *30*, 2233.
(83) Kratky, C.; Dunitz, J. D. *Acta Crystallogr.* **1977**, *B33*, 545.
(84) Kratky, C.; Isenring, H. P.; Dunitz, J. D. *Acta Crystallogr.* **1977**, *B33*, 547.
(85) Ghosh, A. *J. Phys. Chem. B* **1997**, *101*, 3290.
(86) Almlöf, J.; Fischer, T. H.; Gassman, P. G.; Ghosh, A.; Häser, M. *J. Phys. Chem.* **1993**, *97*, 10964.
(87) Chen, B. M. L.; Tulinsky, A. *J. Am. Chem. Soc.* **1972**, *94*, 4144.
(88) Codding, P. W.; Tulinsky, A. *J. Am. Chem. Soc.* **1972**, *94*, 4151.
(89) Risch, N.; Brockmann, H. *Tetrahedron Lett.* **1983**, *24*, 173.
(90) Lötjönen, S.; Michalski, T. J.; Norris, J. R.; Hynninen, P. H. *Magn. Reson. Chem.* **1987**, *25*, 670.
(91) Lötjönen, S.; Hynninen, P. H. *Org. Magn. Reson.* **1983**, *21*, 757.
(92) Lötjönen, S.; Hynninen, P. H. *Org. Magn. Reson.* **1981**, *16*, 304.
(93) Boxer, S. G.; Closs, G. L.; Katz, J. J. *J. Am. Chem. Soc.* **1974**, *96*, 7058.
(94) Linnanto, J.; Korppi-Tommola, J. *Phys. Chem. Chem. Phys.* **2000**, *2*, 4962.
(95) Hashimoto, T.; Choe, Y.-K.; Nakano, H.; Hirao, K. *J. Phys. Chem. A* **1999**, *103*, 1894.
(96) Koepke, J.; Hu, X.; Muenke, C.; Schulten, K.; Michel, H. *Structure* **1996**, *4*, 581.
(97) McLuskey, K.; Prince, S. M.; Cogdell, R. J.; Isaacs, N. W. *Biochemistry* **2001**, *40*, 8783.
(98) Camara-Artigas, A.; Blankenship, R. E.; Allen, J. P. *Photosynth. Res.* **2003**, *75*, 49.
(99) Allen, J. P.; Feher, G.; Yates, T. O.; Komiya, H.; Rees, D. C. In *The Photosynthetic Bacterial Reaction Center. Structure and Dynamics*; Breton, J., Verméglio, A., Eds.; Plenum Press: New York, 1988; pp 5−11.
(100) Koyama, Y.; Umemoto, Y.; Akamatsu, A.; Uehara, K.; Tanaka, M. *J. Mol. Struct.* **1986**, *146*, 273.
(101) Nishizawa, E.-I.; Limantara, L.; Nanjou, N.; Nagae, H.; Kakuno, T.; Koyama, Y. *Photochem. Photobiol.* **1994**, *59*, 229.
(102) Nishizawa, E.-I.; Nagae, H.; Koyama, Y. *J. Phys. Chem.* **1994**, *98*, 12086.
(103) Misono, Y.; Limantara, L.; Koyama, Y.; Itoh, K. *J. Phys. Chem.* **1996**, *100*, 2422.
(104) Vladkova, R. *Photochem. Photobiol.* **2000**, *71*, 71.
(105) Callahan, P. M.; Cotton, T. M. *J. Am. Chem. Soc.* **1987**, *109*, 7001.
(106) Katz, J. J. *Spectrum* **1994**, *7*, 1.
(107) Renge, I.; Avarmaa, R. *Photochem. Photobiol.* **1985**, *42*, 253.
(108) Cotton, T. M.; van Duyne, R. P. *J. Am. Chem. Soc.* **1981**, *103*, 6020.
(109) Visschers, R. W.; van Grondelle, R.; Robert, B. *Biochim. Biophys. Acta* **1993**, *1183*, 369.
(110) Lapouge, K.; Näveke, A.; Gall, A.; Ivancich, A.; Seguin, J.; Scheer, H.; Sturgis, J. N.; Mattioli, T. A.; Robert, B. *Biochemistry* **1999**, *38*, 11115.
(111) Bellacchio, E.; Sauer, K. *J. Phys. Chem. B* **1999**, *103*, 2279.
(112) Mauring, K.; Renge, I.; Sarv, P.; Avarmaa, R. *Spectrochim. Acta* **1987**, *43A*, 507.
(113) Heald, R. L.; Cotton, T. M. *J. Phys. Chem.* **1990**, *94*, 3968.
(114) Nappa, M.; Valentine, J. S. *J. Am. Chem. Soc.* **1978**, *100*, 5075.
(115) Cotton, T. M.; Loach, P. A.; Katz, J. J.; Ballschmiter, K. *Photochem. Photobiol.* **1978**, *27*, 735.
(116) Closs, G. L.; Katz, J. J.; Pennington, F. C.; Thomas, M. R.; Strain, H. H. *J. Am. Chem. Soc.* **1963**, *85*, 3809.
(117) Hartwich, G.; Fiedor, L.; Simonin, I.; Cmiel, E.; Schäfer, W.; Noy, D.; Scherz, A.; Scheer, H. *J. Am. Chem. Soc.* **1998**, *120*, 3675.
(118) Martin, N. H.; Allen, N. W., III.; Brown, J. D.; Kmiec, D. M., Jr.; Vo, L. *J. Mol. Graphics Modell.* **2003**, *22*, 127.
(119) Petke, J. D.; Maggiora, G. M.; Shipman, L. L.; Christoffersen, R. E. *Photochem. Photobiol.* **1982**, *36*, 383.
(120) Petke, J. D.; Maggiora, G. M.; Shipman, L. L.; Christoffersen, R. E. *J. Mol. Spectrosc.* **1978**, *73*, 311.
(121) Petke, J. D.; Maggiora, G. M.; Shipman, L. L.; Christoffersen, R. E. *J. Mol. Spectrosc.* **1978**, *71*, 64.
(122) Petke, J. D.; Maggiora, G. M.; Shipman, L.; Christoffersen, R. E. *Photochem. Photobiol.* **1979**, *30*, 203.
(123) Even, U.; Magen, Y.; Jortner, J.; Levanon, H. *J. Am. Chem. Soc.* **1981**, *103*, 4583.
(124) Even, U.; Magen, Y.; Jortner, J. *J. Chem. Phys.* **1982**, *76*, 5684.
(125) Even, U.; Magen, J.; Jortner, J. *Chem. Phys. Lett.* **1982**, *88*, 131.
(126) Spiedel, D.; Roszak, A. W.; McKendrick, K.; McAuley, K. E.; Fyfe, P. K.; Nabedryk, E.; Breton, J.; Robert, B.; Cogdell, R. J.; Isaacs, N. W.; Jones, M. R. *Biochim. Biophys. Acta* **2002**, *1554*, 75.
(127) Sundholm, D. *Chem. Phys. Lett.* **1999**, *302*, 480.
(128) Parusel, A. B. J.; Grimme, S. *J. Phys. Chem. B* **2000**, *104*, 5395.
(129) Haran, G.; Wynne, K.; Moser, C. C.; Dutton, P. L.; Hochstrasser, R. M. *J. Phys. Chem.* **1996**, *100*, 5562.
(130) Gradinaru, C. C.; Kennis, J. T. M.; Papagiannakis, E.; van Stokkum, I. H. M.; Cogdell, R. J.; Fleming, G. R.; Niederman, R. A.; van Grondelle, R. *Proc. Natl. Acad. Sci. U.S.A.* **2001**, *98*, 2364.
(131) Dedieu, A.; Rohmer, M.-M.; Veillard, A. *Adv. Quantum Chem.* **1982**, *16*, 43.
(132) Linnanto, J. M.; Korppi-Tommola, J. E. I. In *PS2001 Proceedings 12th International Congress on Photosynthesis*; CSIRO Publishing: Collingwood, Australia, 2002.
(133) Matthews, B. W.; Fenna, R. E.; Bolognesi, M. C.; Schmid, M. F.; Olson, J. M. *J. Mol. Biol.* **1979**, *131*, 259.
(134) Fenna, R. E.; Matthews, B. W.; Olson, J. M.; Shaw, E. K. *J. Mol. Biol.* **1974**, *84*, 231.
(135) Tronrud, D. E.; Matthews, B. W. In *Photosynthetic reaction center*; Deisenhofer, J., Norris, J., Eds.; Academic Press: New York, 1993.